Micro-macro model for prediction of local temperature distribution in heterogeneous and two-phase media

PIOTR FURMAŃSKI[*]
MIROSŁAW SEREDYŃSKI
PIOTR ŁAPKA
JERZY BANASZEK

Institute of Heat Engineering, Warsaw University of Technology,
Nowowiejska 25, 00-665 Warszawa, Poland

Abstract   Heat flow in heterogeneous media with complex microstructure follows tortuous path and therefore determination of temperature distribution in them is a challenging task. Two-scales, micro-macro model of heat conduction with phase change in such media was considered in the paper. A relation between temperature distribution on the microscopic level, i.e., on the level of details of microstructure, and the temperature distribution on the macroscopic level, i.e., on the level where the properties were homogenized and treated as effective, was derived. The expansion applied to this relation allowed to obtain its more simplified, approximate form corresponding to separation of micro- and macro-scales. Then the validity of this model was checked by performing calculations for 2D microstructure of a composite made of two constituents. The range of application of the proposed micro-macro model was considered in transient states of heat conduction both for the case when the phase change in the material is present and when it is absent. Variation of the effective thermal conductivity with time was considered and a criterion was found for which application of the considered model is justified.

Keywords: Heterogeneous media; Heat conduction; Micro- macro modeling

[*]Corresponding Author. E-mail: pfurm@itc.pw.edu.pl

Nomenclature

c –   specific heat, J/kgK;

(ρc) –   volumetric specific heat, J/m^{3}K,

G_T –   Green function

h –   specific enthalpy, J/kg

L_m –   latent heat of melting, J/kg

n –   external, normal unit vector

$\mathbf{q}$ –   heat flux, W/m^2,

$\dot{Q}$ –   heat flow rate, W

S –   microstructure function

t –   time

T –   temperature, K

T_m –   melting temperature, K

w_i –   velocity of the solid-liquid interphase

V –   volume

$\mathbf{x}$ –   vector of location, m

ℓ –   characteristic micro-dimension

$\{_-\}$ –   macroscopic value

Greek symbols

α –   heat transfer coefficient

δ –   Dirac function or thickness of a composite

ε –   volume fraction of the constituent

θ –   structure function

ϕ –   microstructure function

λ –   thermal conductivity, W/m^{2}K

ρ –   density, kg/m^3

τ –   dummy variable corresponding to time

ψ –   microstructure function

Ω –   configuration of components distribution

Subscripts

c –   convective

e –   external surface

ef –   effective

k –   type of constituent

m –   matrix

f –   fibre

l –   liquid

r –   reference value

s –   solid

ST –   time independent form of the respective function

1   Introduction

Heterogenous media are characterized by complex form of constituent distribution (e.g,. composites, thermal insulations, building materials, soil) [6,7]. Heat transfer processes in these media are sometimes assisted by phase transformations, which lead to formation and variation in the media microstructure (e.g., two-phase region known as „mushy zone" in solidifying alloys) [1,8]. Numerical analysis of heat and mass transfer in heterogeneous media with highly dispersed constituents is very tedious and is usually out of nowadays computing capabilities [4,11]. Therefore, in the mathematical description and numerical simulation of transfer processes occurring in heterogeneous media it is common to replace a medium with locally stepwise varying properties with a continuous (effective) medium with constant or smoothly varying macroscopic (effective) properties [5]. Such two-scale type approach allows for a significant simplification and quicker analysis of transfer processes in heterogeneous media. In processes where the structure is developed, i.e., alloy solidification, or local thermal stresses affect durability of a material local (on the microscopic level) temperature, the species concentration or thermal deformations are of importance [9]. Then a question can be raised if from the knowledge of medium microstructure and macroscopic distributions of temperature, species concentration or deformation obtained on the macroscopic level, i.e., using the effective medium approach it is possible to derive information about these distributions on the local (microscopic) level [9]. In the case of microstructure formation the question is posed of what kind of the microstructure is developed and how it evolves in time. A few approaches to micro-macro modelling of microstructure formation in crystallizing alloys with a different success were proposed in literature [2,3,9,10].

In the paper two problems were analyzed. The first one refers to determination of the local temperature distribution from the macroscopic one. The second problem is related to limitations placed on scope of application of the effective properties, i.e., in what case the effective medium approach is applicable. In both problems it was assumed that the heterogeneous medium was made from regularly arranged cylindrical inclusions (fibres) in a matrix material. The heat transfer process was limited to heat conduction but the transient state of heat transfer was considered and in some cases the phase change occurring in the fibres was accounted for. Initially a comparison has been carried out between temperature distribution in a heterogeneous material obtained directly from numerical simulation with step-wise vary-

ing properties with temperature distribution obtained via solution of the macroscopic temperature distribution using effective medium approach. In the second part of the paper the effective thermal conductivity was calculated from transient temperature and heat flux distributions. It was studied for what time, counting from the beginning of the heat transfer process, the macroscopic approach could be used as justified by the observed, constant value of the effective thermal conductivity.

2   Relation between microscopic and macroscopic temperature in the heterogeneous medium

Heat transfer in a heterogeneous medium with possible phase change appearing in the constituents, in absence of convection and thermal radiation as well as for known distribution of constituents is described by the following equation [1]:

$$\partial_t(\rho_k h_k) = \nabla \cdot \mathbf{q}_k \ , \tag{1}$$

where the symbol k denotes the respective constituent and in particular corresponds to solid s or liquid phase l, i.e. $k = s, l$; ∂_t is the time derivative, ρ_k and h_k are the density and specific enthalpy, respectively while the symbol $\mathbf{q}_k$ stands for the heat flux vector in kth constituent.

Balance of energy should be satisfied not only in interior of constituents but also at the interfaces between them. In particular for a constituent undergoing phase transformation it should be satisfied at the liquid/solid interphase, which moves with a velocity $\mathbf{w_i}$, i.e.:

$$[-\rho_s h_s \mathbf{w}_i + \mathbf{q}_s] \cdot \mathbf{n}_s + [-\rho_l h_l \mathbf{w}_i + \mathbf{q}_l] \cdot \mathbf{n}_l = 0 \ , \tag{2}$$

where $\mathbf{w}_i$ is the velocity of the solid-liquid interphase, $\mathbf{n}_s$, $\mathbf{n}_l$ are the external, normal unit vectors to solid or liquid interphase.
After rearrangement and introduction of the latent heat of the phase change Eq. (2) leads to the expression

$$(\mathbf{q}_s - \mathbf{q}_l)\mathbf{n}_s = -\rho_s(h_l - h_s)\mathbf{w}_i \cdot \mathbf{n}_s = -\rho_s L_m \mathbf{w}_i \cdot \mathbf{n}_s \ . \tag{3}$$

Additionally it was assumed that at the liquid/solid interphase the melting (freezing) temperature is held $T_s = T_l = T_m$ and that the heat flux $\mathbf{q}$ in each constituent (phase) is described by the Fourier law with assumed isotropic properties of materials:

$$\mathbf{q}_k = -\lambda_k \nabla T \ , \tag{4}$$

where λ_k is the thermal conductivity of kth constituent.

All quantities appearing in the above equations, including specific heats and thermal conductivities are dependent on location $\mathbf{x}$ and on the way (configuration) the constituents are distributed in the heterogeneous material, which is described by the symbol Ω.

Before the macroscopic description is used it is convenient to introduce the generalized function [5]

$$f(t, \mathbf{x}|\Omega) = \sum_k \theta(t, \mathbf{x}|\Omega) f_k(t, \mathbf{x}|\Omega) , \qquad (5)$$

which allows to write all equations in one, generalized way accounting for the presence of many constituents (phases) in the material. The function θ is known as the structure function and is defined in the following way [1]:

$$\theta_k = \theta_k(t, \mathbf{x}|\Omega) = \begin{cases} 1 & \text{for} \quad \mathbf{x} \in \mathbf{V}_k , \\ 0 & \text{for} \quad \mathbf{x} \notin \mathbf{V}_k \end{cases} \qquad (6)$$

where V_k denotes the volume of kth constituent (here solid and liquid phases are treated as distinct constituents). The structure function satisfies the following relations [1]:

$$\sum_k \theta_k(t, \mathbf{x}) = 1 , \qquad (7)$$

$$\partial_t \theta_k + \mathbf{w_i} \cdot \nabla \theta_k = 0 , \qquad (8)$$

$$\nabla \theta_k = -\mathbf{n}_k \delta(\mathbf{x}, \mathbf{x}_i) , \qquad (9)$$

where the symbol δ denotes the Dirac pseudo-function, $\mathbf{x_i}$ describes location of the solid/liquid interphase while the vector $\mathbf{n}_k$ is a unit, external vector normal to boundary of kth constituent (phase).

Any function f dependent of the constituent configuration can be statistically averaged over a set of allowed distributions Ω. The average '·' (macroscopic value) denotes therefore the statistically awaited average. If the function f corresponds to the structure function θ_k then:

$$\{\theta_k(t, \mathbf{x})\} = \varepsilon_k(t, \mathbf{x}) . \qquad (10)$$

Variation of temperature in a heterogeneous material is affected by heat conduction in the constituents, energy accumulation and generation (or absorption) of heat due to the phase transformation. The macroscopic energy equation, independent of the particular distribution of constituents, can be

obtained via multiplying the microscopic energy Eq. (1) by the structure function θ_k. This leads to the equation

$$\partial_t(\theta_k \rho_k h_k) + \nabla \cdot (\theta_k \mathbf{q}_k) = [\partial_t \theta_k]\rho_k h_k + \nabla\theta_k \cdot \mathbf{q}_k \; . \qquad (11)$$

The r.h.s. of this equation can be transformed, using expression (2) to the form

$$\partial_t(\theta_k \rho_k h_k) + \nabla \cdot (\theta_k \mathbf{q}_k) = [\rho_k h_k(-\mathbf{w}_i) + \mathbf{q}_k] \cdot \nabla\theta_k \; . \qquad (12)$$

The Eq. (12), valid for each constituent (phase), can be subsequently summed up over all constituents giving

$$\partial_t(\rho h) + \nabla \cdot \mathbf{q} = 0 \; . \qquad (13)$$

If the volumetric specific heats (products of density and specific heats) as well as the latent heat of melting are assumed constant then the energy equation can be cast to the form

$$\partial_t(\rho c T) + \nabla \cdot \mathbf{q} = \mathbf{w}_i L_f \nabla\theta_l \, . \qquad (14)$$

The Eq. (13), when statistically averaged, leads to the macroscopic form of the energy equation:

$$\partial_t\{\rho h\} + \nabla \cdot \{\mathbf{q}\} = 0 \; . \qquad (15)$$

Using the same assumptions as earlier stated Eq. (14) can be expressed, after introduction of Eq. (1) and averaging in its macroscopic form:

$$\partial_t\{\rho c T\} + \nabla \cdot \{\mathbf{q}\} = -L_m \partial_t \varepsilon_l \; , \qquad (16)$$

where ε_l is the volume fraction of the fluid. When the enthalpy formulation of the energy equation, Eq. (15), is utilized in analysis the location of solid/liquid interphase on the macroscopic level is determined from the relation between the enthalpy and melting temperature T_m.

In order to solve the macroscopic energy equation relations between the mean values of $\{\rho h\}$ and $\{\mathbf{q}\}$ appearing in Eqs. (15) or (7) with the macroscopic temperature $\{T\}$ are needed. They could be easily derived if the relations between the microscopic T and macroscopic one $\{T\}$is known. In order to find these relations the generalized form of the Fourier law

$$\mathbf{q} = -\lambda \nabla T \qquad (17)$$

was introduced in the energy equation (1), where the thermal conductivity, λ, is defined in the following way:

$$\lambda = \sum_{k=1}^{4} \theta_k(t, \mathbf{x}|\Omega)\lambda_k \ . \tag{18}$$

The microscopic energy equation was then transformed to the form

$$\rho_r c_r \partial_t T - \lambda_r \nabla^2 T - F_T = 0 \ , \tag{19}$$

where the source function F_T has been defined as

$$F_T = \nabla \cdot (\lambda' \nabla T) - \partial_t(\rho h - \rho_r c_r h) \tag{20}$$

and

$$\lambda' = \lambda - \lambda_r \ , \tag{21}$$

where the subscript r denotes the reference value.

The boundary condition, assumed on the external boundary of the heterogeneous material, was written as

$$\mathbf{q} \cdot \mathbf{n}_e - \alpha_c(T - T_\infty) = f_T \ , \tag{22}$$

where the ambient temperature, T_∞, convective heat transfer coefficient, α_c and the function f_T, depend on location and time but are independent of the way the constituents are distributed in the material, i.e., on Ω and $\mathbf{n}_e$ is the unit vector normal to the external surface. The above equations were supplemented with the initial condition in the form

$$T(t = 0, \mathbf{x}|\Omega) = T_o(\mathbf{x}) \ . \tag{23}$$

Subsequently the Green function, G_T, as defined by the set of the following equations, has been introduced:

$$\lambda_r \nabla^2 G_T + \partial_x(\mathbf{x}, \mathbf{y})\partial_t(t, \tau) = -\rho_r c_r \partial_t G_T \quad \text{for} \quad \mathbf{x} \in V \ , \tag{24}$$

$$(\lambda_r \nabla G_T) \cdot \mathbf{n}_e - \alpha_c G_T = 0 \quad \text{for} \quad \mathbf{x} \in A \ ,$$

$$G_T(t, \mathbf{x}; \tau, \mathbf{y}) = 0 \quad \text{for} \quad t \leq \tau \ ,$$

where V is the the medium volume.

Using the Green function theory Eq. (19) can be formally solved for the local temperature:

$$T = \int_V \rho_r c_r G_T T_o dV - \int_0^t \int_V \nabla G_T \cdot [\lambda'' \nabla T] dV' d\tau +$$

$$- \int_0^t \int_V G_T \partial_\tau (\rho h - \rho_r c_r T) dV' d\tau +$$

$$+ \int_0^t \int_A G_T [f_T] dA' d\tau \ . \tag{25}$$

Statistically averaging of the above equation and its subsequent subtraction from the Eq. (25) leads to the following relation between the microscopic and macroscopic temperatures:

$$T = \{T\} - \int_0^t \int_V \nabla G_T \cdot \big[(\lambda' \nabla T - \{\lambda' \nabla T\})\big] dV' d\tau +$$

$$- \int_0^t \int_V G_T \partial_t \big[(\rho h - \rho_r c_r T) - \{\rho h - \rho_r c_r T\}\big] dV' d\tau \ . \tag{26}$$

The volumetric specific enthalpy ρh is dependent on the material temperature and can be expanded in series around the macroscopic temperature. The differences between the microscopic and macroscopic enthalpy appearing in this expansion can be introduced into Eq. (26). This procedure leads to the following form of the latter equation:

$$T = \{T\} + S + \int_0^t \int_V \phi \cdot \nabla' \{T\} dV' d\tau + \int_0^t \int_V \psi \partial_\tau \{T\} dV' d\tau \ , \tag{27}$$

where S, ϕ and ψ, which are subsequently called the microstructure functions, describe differences between the local and macroscopic temperature caused by presence of heat sources or the space and time variation in the macroscopic temperature. After substitution of the relation (27) into Eq. (26) the integro-differential equations for the unknown 'microstructure' functions ϕ, ψ, S were derived:

$$\phi = \int_0^t \int_V \nabla G_T \cdot \big[(\lambda'(\mathbf{1}\delta_t \delta_x + \nabla \phi) - \{\lambda'(\mathbf{1}\delta_t \delta_x + \nabla \phi)\})\big] dV' d\tau +$$

$$- \int_0^t \int_V \nabla G_T \big[(\rho^o c^o \partial_\tau \phi - \{\rho^o c^o \partial_\tau \phi\}) +$$

$$+ ((\mathbf{w}_i \cdot \nabla \theta_s) \phi - \{(\mathbf{w}_i \cdot \nabla \theta_s) \phi\}) \Delta(\rho^o c^o) - \rho_r c_r \partial_\tau \phi\big] dV' d\tau \ , \tag{28}$$

where $\mathbf{1}$ is the unit second order tensor, and, and δ_x, δ_t denote Dirac functions in respect to location and time.

$$\psi = \int_0^t \int_V \nabla G_T \cdot \left[(\lambda' \nabla \psi) - \{\lambda' \nabla \psi\}\right] dV' d\tau +$$
$$-\int_0^t \int_V \nabla G_T \cdot \left[(\rho^o c^o (\delta_x \delta_t + \partial_\tau \psi) - \{\rho^o c^o (\delta_x \delta_t + \partial_\tau \psi)\}) + \right.$$
$$\left. +((\mathbf{w}_i \cdot \nabla \theta_s)\psi - \{(\mathbf{w}_i \cdot \nabla \theta_s)\psi\})\Delta(\rho^o c^o) - \rho_r c_r \partial_\tau \psi\right] dV' d\tau , \quad (29)$$

$$S = \int_0^t \int_V \nabla G_T \cdot \left[(\lambda' \nabla S) - \{\lambda' \nabla S\}\right] dV' d\tau +$$
$$-\int_0^t \int_V G_T \left[(\rho_o c^o \partial_\tau S - \{\rho_o c^o \partial_\tau S\}) + ((\mathbf{w}_i \cdot \nabla \theta_s) - \{(\mathbf{w}_i \cdot \nabla \theta_s)\}\Delta(\rho^o h^o)\right.$$
$$\left. +((\mathbf{w}_i \cdot \nabla \theta_s)S - \{(\mathbf{w}_i \cdot \nabla \theta_s)S_T\})\Delta \rho^o c^o - \rho_r c_r \partial_\tau S\right] dV' d\tau . \quad (30)$$

The superscript 'o' in Eqs. (28)–(30) denotes determination of the considered function for the macroscopic temperature $\{T\}$ while the expression $\Delta(\rho^o c^o)$ is related to difference in the volumetric specific heats of the constituents undergoing the phase change.

Substitution of the expression (26) into the averaged terms appearing in the macroscopic forms of the energy equation, Eqs. (15) or (16), leads to the following relations between the macroscopic heat flux and volumetric specific enthalpy on one side and the macroscopic temperature on the other side:

$$\{\mathbf{q}\} = -\mathbf{q}_{ST} - \int_0^t \int_V \lambda_{ef} \cdot \nabla'\{T\} dV' d\tau - \int_0^t \int_V \gamma_{ef} \partial_\tau \{T\} dV' d\tau , \quad (31)$$

$$\{\rho h\} = \{\rho^o h^o\} + h_{ST} + \int_0^t \int_V \varsigma_{ef} \cdot \nabla'\{T\} dV' d\tau \int_0^t \int_V \mu_{efj} \partial_\tau \{T\} dV' d\tau ,$$
$$(32)$$

where the macroscopic (effective) properties are defined by the formulae:

$$\lambda_{ef} = \{\lambda(\mathbf{1}\delta_x \delta_t + \nabla \phi)\} ,$$

$$\gamma_{ef} = \{\lambda \nabla \psi\} ,$$

$$\mathbf{q}_{ST} = \{\lambda \nabla S\} ,$$

$$h_{ST}\{\rho^o c^o S\} ,$$

$$\varsigma_{ef} = \{\rho^o c^o \phi\} \,,$$

$$\mu_{ef} = \{\rho^o c^o \psi\} \,.$$

The term $\mathbf{q}_{ST}$ shows the effect of local, temperature dependent, heat sources existing at solid/liquid interface on the heat flux and the terms containing the effective properties h_{ST}, ς_{Tef} and μ_{Tef}, are responsible for the additional heat accumulation in the material. The heat sources appearing at the boundaries of constituents undergoing phase transformations locally deform temperature distribution and contribute to the additional heat fluxes and heat accumulation in the material.

3   Simplified relation between the microscopic and macroscopic temperatures in a heterogeneous medium following from separation of scales

If the greatest micro-dimension ℓ, e.g., the mean distance between inclusions in the heterogeneous material, is smaller than the smallest macro-dimension associated with variation of the macroscopic temperature in the material the significant simplification can be obtained based on this scale separation. The functions ϕ, ψ, S can be expanded into the infinite series of growing powers of the micro-dimension ℓ , i.e.,
– for function ϕ:

$$\phi(t, \mathbf{x}; \tau, \mathbf{y}\,|\Omega)/\ell^2 = \phi_0(t, \mathbf{x}\,|\Omega)\delta(t, \tau)\delta(\mathbf{x}, \mathbf{y})+$$
$$+\ell\phi_1(t, \mathbf{x}\,|\Omega)\delta(t, \tau)\nabla\delta(\mathbf{x}, \mathbf{y}) + O(l^2) \,, \tag{33}$$

– for function S:

$$S(t, \mathbf{x}; \tau, \mathbf{y}\,|\Omega)/\ell^2 = S_0(t, \mathbf{x}\,|\Omega)\delta(t, \tau)\delta(\mathbf{x}, \mathbf{y})+$$
$$+\ell S_1(t, \mathbf{x}\,|\Omega)\delta(t, \tau)\nabla\delta(\mathbf{x}, \mathbf{y}) + O(l^2) \,, \tag{34}$$

– for function ψ:

$$\psi(t, \mathbf{x}; \tau, \mathbf{y}\,|\Omega)/\ell^2 = \psi_0(t, \mathbf{x}\,|\Omega)\delta(t, \tau)\delta(\mathbf{x}, \mathbf{y})+$$
$$+\ell\psi_1(t, \mathbf{x}\,|\Omega)\delta(t, \tau)\nabla\delta(\mathbf{x}, \mathbf{y}) + O(l^2) \,. \tag{35}$$

The scale separation is valid when the first terms on the r.h.s. of the above expansions are remained. This corresponds to the assumption that gradients

and time derivatives of the macroscopic temperature are varying slowly in space and time and therefore the scales associated with them are much greater than the micro-dimension ℓ.

When the expansions of Eqs. (33)–(35) are substituted into Eqs. (27)–(30) and condition for separation of scales is invoked, the following relation between the microscopic and macroscopic temperatures is received

$$T = \{T\} + \ell S_0 + \ell\big[\phi_0 \cdot \nabla\{T\}\big] + O(\ell^2) \tag{36}$$

while the integro-differential equations for the functions ϕ, S are reduced to the form

$$\phi_0 = -\int_V \nabla G_T \cdot \big[\lambda'(\mathbf{1} + \nabla\phi_0) - \{\lambda'(\mathbf{1} + \nabla\phi_0)\}\big]dV', \tag{37}$$

$$S_0 = \int_0^t \int_V \nabla G_T \cdot \big[(\lambda'\nabla S_0) - \{\lambda'\nabla S\}\big]dV'd\tau +$$
$$- \int_0^t \int_V G_T\big[(\mathbf{w}_i \cdot \nabla\theta_s) - \{(\mathbf{w}_i \cdot \nabla\Theta_s)\}\big]\Delta(\rho^o h^o)dV'd\tau . \tag{38}$$

Also the equivalent differential form of the above equations can be derived and is given by the formulae:

$$\nabla \cdot \lambda\nabla\phi = 0 , \tag{39}$$

$$\lambda\nabla\phi \cdot \mathbf{n}|_A = \lambda_{ef} \cdot \mathbf{n}|_A , \tag{40}$$

$$\nabla \cdot \lambda\nabla S + \big[(\mathbf{w}_i \cdot \nabla\theta_s) - \{(\mathbf{w}_i \cdot \nabla\theta_s)\}\big]\Delta(\rho^o h^o) = 0 , \tag{41}$$

$$\lambda\nabla S \cdot \mathbf{n}|_A = \lambda'\nabla S \cdot \mathbf{n}|_A , \tag{42}$$

where A denotes the external area of the material.

In a similar way after substitution of these expansions into expression (31) and (32) the following relations for the macroscopic heat flux and mean volumetric specific enthalpy are derived:

$$\{\mathbf{q}\} = -\lambda_{ef} \cdot \nabla\{T\} , \tag{43}$$

$$\{ph\} = \{\rho^o h^o\} . \tag{44}$$

The effective thermal conductivity appearing in the relation (43), corresponding to the Fourier law for the macroscopic quantities, is defined in the following way:

$$\lambda_{ef} = \{\lambda(\mathbf{1} + \nabla\phi_0)\} . \tag{45}$$

Equations (37)-(42) are based on the local coordinates related to the macroscopic ones by the following formula:

$$\xi = \mathbf{x}/\ell \, ,$$

where the origin of these local coordinates is placed in the nearest characteristic point associated with the medium microstructure, e.g., in the centre of inclusion.

In order to illustrate application of this two-scale model the problem of heat conduction in the composite shown in Fig.1 was considered. Different temperatures T_1 and T_2 are applied to the left and right surfaces of the composite domain. The other surfaces are treated as thermally insulated.
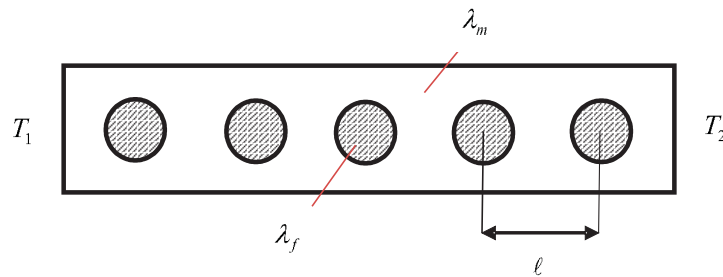
Figure 1: Geometry of a composite for determination of temperature distribution: ℓ is the characteristic microdimension and λ_m, λ_f are the matrix and fibre thermal conductivities, respectively.

In absence of the phase change Eqs. (39) and (40) were solved for the microstructure vector function ϕ. As the macroscopic heat flow occurs in direction x (from higher temperature T_2 to lower T_1) then the component ϕ_x of this function is only of interest and its form is shown in Fig. 2. In the steady state of heat conduction the gradient of macroscopic temperature $\{T\}$ is constant for the given boundary conditions and the formula from Eq. (36) was used to calculate an approximate microscopic temperature distribution. The latter was compared with the temperature distribution obtained from the solution of the original problem on the microscopic level. The results show very good accuracy of the results predicted via the macroscopic problem (reconstructed distribution) with the exact ones (real distribution) – Fig. 3.
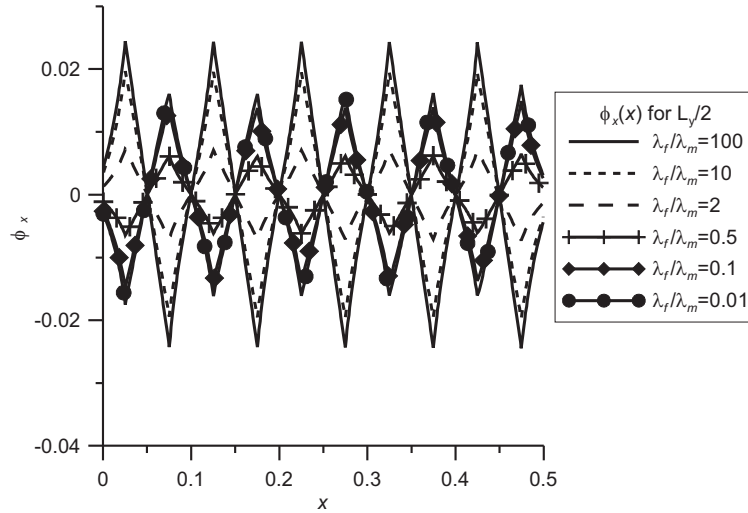
Figure 2: Variation of the x component of the microstructure function λ_x with distance and ratio of fibre/matrix thermal conductivities.
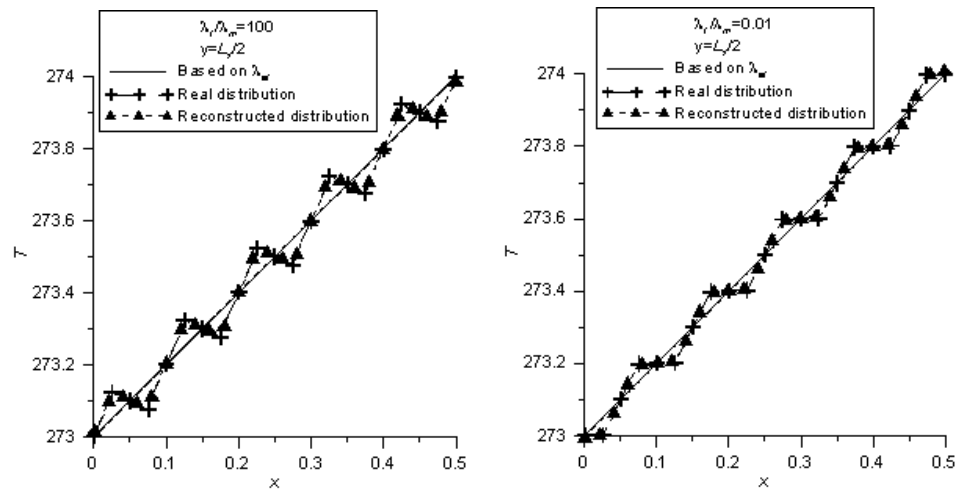

Figure 3: Comparison of the microscopic temperature distribution along the centre line of the composite obtained in the exact way (real distribution) and using Eq. (36) based on the macroscopic temperature distribution (reconstructed distribution) for two fibre/matrix thermal conductivity ratios.

4 Limits of application of two-scale model following from transient states of heat conduction -

It is interesting to find when the approximation discussed at the end of the last chapter is valid, i.e., when the microscopic temperature can be approx-

imated by the formula (36), in which the macroscopic temperature is used. It can be noticed that also the microscopic and macroscopic temperature are dependent on location expressed by the vector $\mathbf{x}$ and time t the functions ϕ, S, appearing in Eq. (36), do not depend on time. Therefore also the effective thermal conductivity, defined in Eq. (45), does not depend on time. It can thus serve as way to verify validity of the discussed assumption.

The effective thermal conductivity of the composite can be found in the following way. The divergence of the product of heat flux vector $\mathbf{q}$ and the location vector $\mathbf{x}$ was integrated over the whole composite domain, V, to give

$$\int_V \nabla \cdot (\mathbf{q}\mathbf{x})dV = \int_V \mathbf{x}\nabla \cdot \mathbf{q}dV + \int_V \mathbf{q}dV \ . \tag{46}$$

After substitution of the energy equation, Eq. (1), and converting the volume integral on the l.h.s. of the above equation to the surface integral, the Eq. (46) was transformed to the form

$$\oint_A (\mathbf{q} \cdot \mathbf{n})\mathbf{x}dA = -\int_V \mathbf{x}\frac{\partial (\rho h)}{\partial t}dV + \int_V \mathbf{q}dV \ , \tag{47}$$

where the symbol $\mathbf{n}$ denotes the external unit vector normal to the domain surface. The relation between the heat flux vector and temperature, following from the Fourier law, was subsequently substituted into the second term of Eq. (47) and the volume integral over the temperature gradient changed into the surface integral giving

$$\oint_A (\mathbf{q} \cdot \mathbf{n})\mathbf{x}dA = -\int_V \mathbf{x}\frac{\partial (\rho h)}{\partial t}dV + \lambda_{ef} \oint_A T\mathbf{n}\, dA \ . \tag{48}$$

The formula of Eq. (48) can be applied to the rectangular domain – see Fig. 4. Depending on the location of the origin of the x coordinate axis two formulas for the effective thermal conductivity can be obtained:

$$\lambda_{ef,L} = \frac{\dot{Q}_2\delta}{(T_1 - T_2)A} - \frac{\int_V \partial_t(\rho h)}{(T_1 - T_2)}xdx \ , \tag{49}$$

$$\lambda_{ef,R} = \frac{\dot{Q}_1\delta}{(T_1 - T_2)A} + \frac{\int_V \partial_t(\rho h)}{(T_1 - T_2)}xdx \ , \tag{50}$$

where A is the lateral area of the composite sample. The first formula corresponds to the origin of coordinates located on the left surface of the composite while the second one the origin of coordinates located on the right
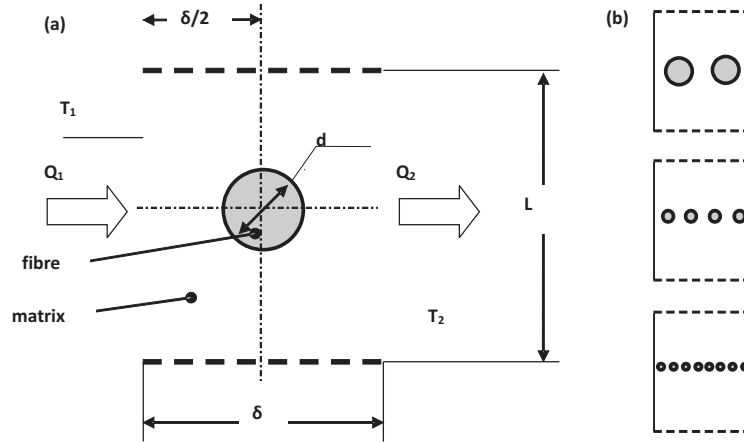
Figure 4: Structure of the considered composite material for evaluation of the effective thermal conductivity: δ – composite thickness, L – composite height, T_1, T_2 – temperatures on the left and right surface of the composite, Q_1, Q_2 – heat flux through the left and right surface of the composite, d – fibre diameter.

surface of the composite. The symbols $\dot{Q}_1$ and $\dot{Q}_2$ describe heat flow rate through left and right surface of the composite, respectively – see Fig. 4. The volumetric specific enthalpy of the constituents was expressed with the formula

$$(\rho h) = c(T - T_{ref}) + \varepsilon_l L_m \ , \tag{51}$$

where ε_l is the fraction of the solid phase in the elementary volume, L_m – latent heat of melting and T_{ref} is the reference temperature.

In the further analysis a composite made of two constituents a matrix with the thermal conductivity λ_m and cylindrical fibers with the thermal conductivity λ_f were assumed. The fibres were unidirectionally aligned and dispersed in the matrix in the regular fashion as shown in Fig. 4. Heat conduction occurred in the direction perpendicular to fibres. Moreover, the fibre material could undergo the phase change. Initial geometry of the composite was shown on the l.h.s. part (a) of Fig. 4. Subsequently the new structures of the composite were derived from this original structure by increasing the number of fibers from 1 to 8 with the respective decrease in distance between them – see Fig. 4. During this process of increasing the dispersion of fibres in the matrix, the total volume fraction of the fibre material in the composite was not changed. Constant but different temperatures T_1, T_2 were assumed on the opposite side of the composite domain. The

other side were thermally insulated. The boundary conditions corresponded
to these for which thermal conductivity of materials is measured using the
steady state method. The energy equation corresponding to Eq. (1), was
solved using the finite volume method with unstructured mesh and applica-
tion of the implicit Euler scheme for integration in time. In the numerical
simulations carried out with commercial software [13] additional data were
also assumed: the volume fraction of fibres was $\varepsilon_f = 0.2$, composite thick-
ness $\delta = 0.1$ m and the latent heat of melting for the fibre material was
assumed to be $L_m = 250$ kJ/kg. The left surface of the composite was
kept at temperature $T_1 = 300$ K while the right surface at temperature
$T_2 = 290$ K. The combination of thermal properties, listed in the table
above, were considered.

Table 1: Thermal properties of composite constituents.

Case	λ_m, W/m K	$(\rho c)_m$, MJ/m³K	λ_f, W/m K	$(\rho c)_f$, MJ/m³K
a	1	1.596	0.3	2.175
b	1	2	0.3	2
c	1	1.596	1	2.175

Subsequently the numerical results were expressed in the dimensionless
form, i.e., the ratio of the effective to matrix thermal conductivity and
the dimensionless time – Fourier number. The latter number: $\text{Fo} = \frac{a_m t}{\ell^2}$,
was based on the thermal diffusivity of the matrix material a_m while the
characteristic length l was assumed to be the distance between fibres.

No phase transformation At the first no phase transformation was
considered in the composite. In all carried out calculations it was found that
that the effective thermal conductivity values obtained from independent
relations (49) and (50) assumed the identical values already after two time
steps – see, eg., Fig. 5.

For the cases (a) and (b) the effective thermal conductivity, after the
initial stage of an increase attained the maximum value and then decreased
with time tending to the asymptotic value for long times after the process
had been initiated – Figs. 6a and 7a. During the period of decrease the
effective thermal conductivity was different for different dispersion of fibre
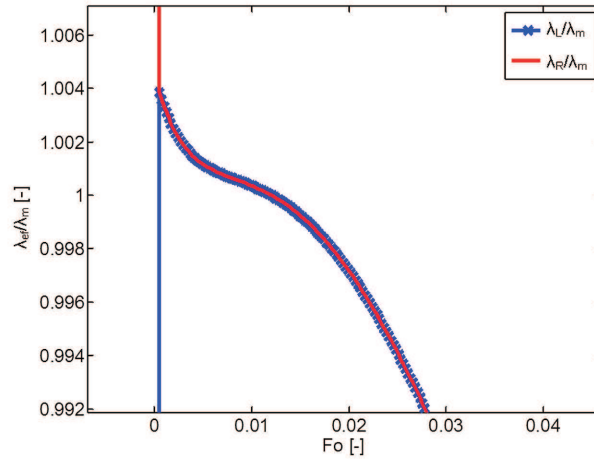material in the composite. Irrespective of a degree of dispersion of the

Figure 5: The effective conductivity of the composite at the initial stage of heat transfer versus Fourier number – case (a): λ_m – thermal conductivity of the matrix, $\lambda_L = \lambda_{ef,L}$, $\lambda_R = \lambda_{ef,R}$ – see Eqs (49) and (50).
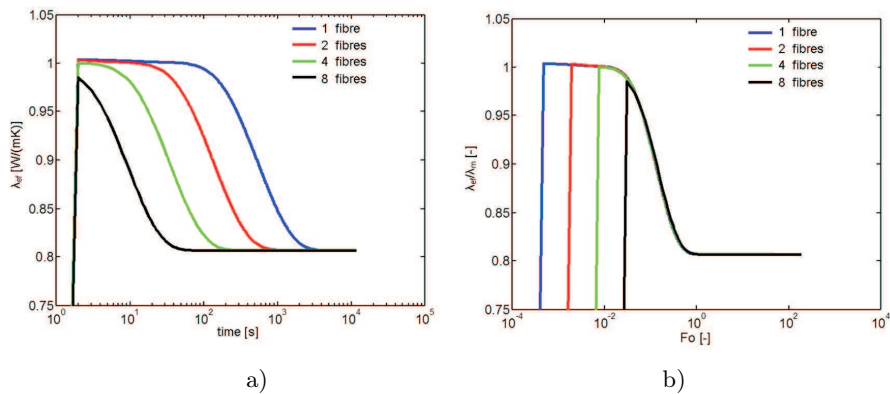

a)   b)

Figure 6: The effective thermal conductivity (or the ratio of the effective to matrix conductivities) versus time (Fourier number) for no phase transformation and different degree of dispersion of fibre material for the case (a) of properties combination.

fiber material the asymptotic value of λ_{ef} was the same. Moreover, it was observed that this asymptotic value is attained quicker for the higher degree of dispersion of the matrix material.

It was then noticed that, irrespective of the different degree of dispersion, all effective thermal conductivity values, after different initial time follow
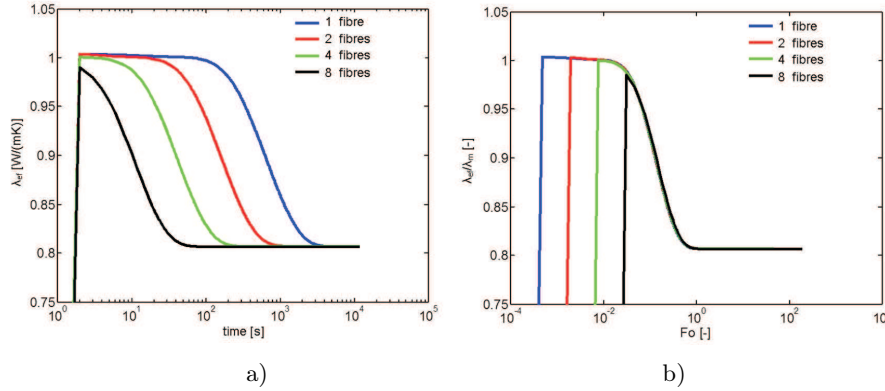
a)   b)

Figure 7: The effective thermal conductivity (or the ratio of the effective to matrix conductivities) versus time (Fourier number) for no phase transformation and different degree of dispersion of fibre material for the case (b) of properties combination.

the same trend and attain the same dimensionless values of λ_{ef}/λ_m for the same Fourier number close to 1 – see Figs. 6b, 7b. This result was obtained for different thermal conductivities of composite constituents no matter whether the volumetric specific heat were different – case (a) or the same – case (b).

The calculations were also carried out for the case (c) when the volumetric specific heats of composite constituents were different but their thermal conductivities the same. Then the effective thermal conductivity, equal to 1 W/m K, was attained already at the very short times after the process initialization not being affected by the fibre dispersion – see Fig. 8.

Nonisothermal phase change   At the second series of calculations the non-isothermal phase change was considered. The phase change was assumed to occur within 1 K around the temperature 295 K. It was also assumed that the mass fraction of the solid phase is a linear function of temperature and the latent heat of melting is $L_m = 250$ kJ/kg. The fraction of melted fibre material is shown in Fig. 10.
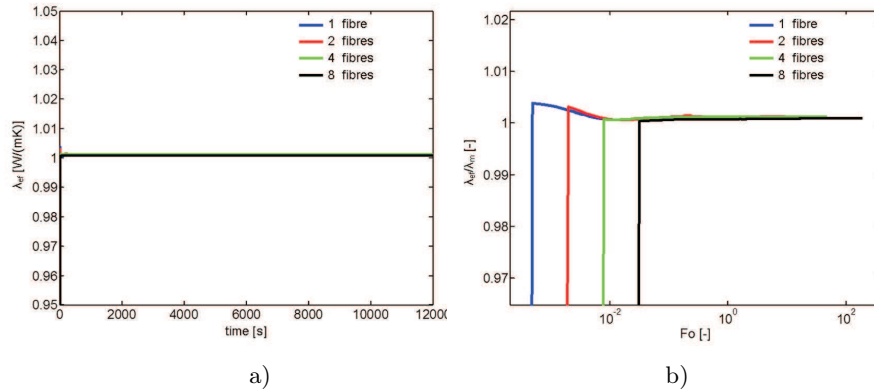
Figure 8: The effective thermal conductivity (or the ratio of the effective to matrix conductivities) versus time (Fourier number) for no phase transformation and different degree of dispersion of fibre material for the case (c) of properties combination.
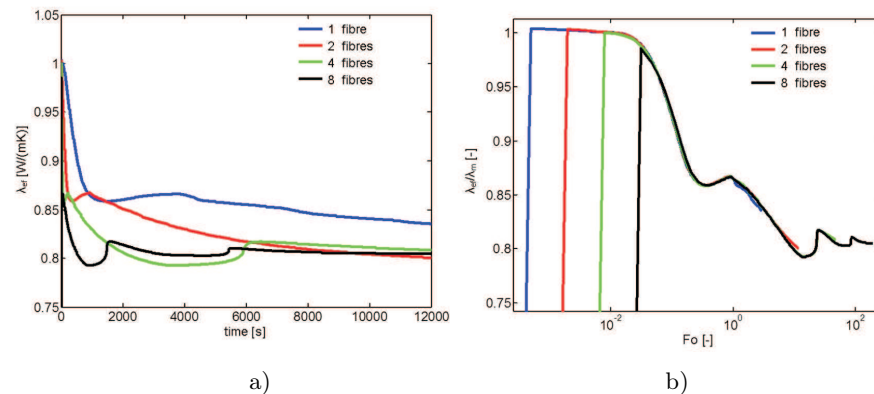

Figure 9: The effective thermal conductivity (or the ratio of the effective to matrix conductivities) versus time (Fourier number) for nonisothermal phase transformation and different degree of dispersion of fibre material for the case (a) of properties combination.

The calculated effective thermal conductivity was found to vary with time but gradually tended to the constant asymptotic value – see Figs. 9a and 11a. The same behavior as for no phase change was found, i.e., the asymptotic values were attained earlier for the higher degree of the fibre dispersion. However oscillations in λ_{ef} for low times were observed independent of the case whether the volumetric specific heats of the composite constituents were different – case (a) or the same – case (b). These oscillations, with

Figure 10: The melted fibre material for the case of the nonisothermal phase change and different degree of dispersion (a) 8 fibres (after $t = 365$ s), (b) 16 fibres (after $t = 401$ s), (c) 32 fibres (after $t = 726$ s), (d) 64 fibers (after $t = 743$ s).

decreasing amplitude were also seen for Fo $< 10^2$ when the dimensionless values were utilized – see Figs. 9b and 11b. The dimensionless time for which the asymptotic value of the effective thermal conductivity was again found for the Fourier number close to unity.
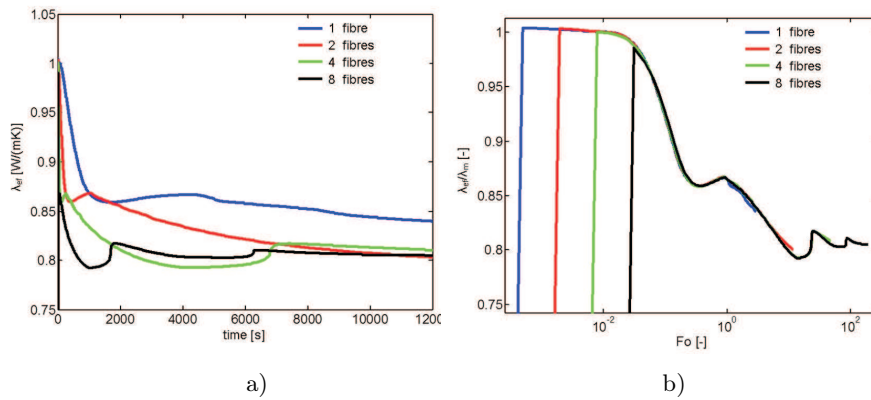

Figure 11: The effective thermal conductivity (or the ratio of the effective to matrix conductivities) versus time (Fourier number) for non-isothermal phase transformation and different degree of dispersion of fibre material for the case (b) of properties combination.

If the thermal conductivities of composite constituents were the same but the volumetric specific heat differed then, for the nonisothermal phase transformation, the asymptotic value of $\lambda_{ef} = 1$ W/m^{2}K was attained for much lower values of the Fourier number corresponding to 0.1. No oscillations in

calculations were observed that were so characteristic for different thermal conductivities of constituents.

The isothermal phase change In the last series of calculations the isothermal phase change was assumed with the melting temperature $T_m = 295$ K. The results of simulations for different thermal conductivities and specific heats of composite constituents are shown in Fig. 12. The results are very similar to those obtained for the nonisothermal phase change with the same, observable oscillations being damped for Fo $\geq 10^2$.

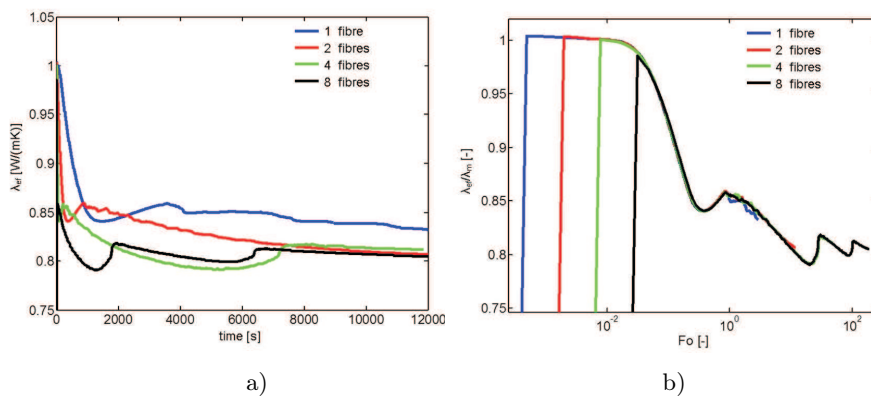a)   b)

Figure 12: The effective thermal conductivity (or the ratio of the effective to matrix conductivities) versus time (Fourier number) for the isothermal phase transformation and different degree of dispersion of fibre material for the case (a) of properties combination.

5   Conclusions

It was shown that the microscopic temperature distribution in the heterogeneous medium, in which transient heat conduction with phase change is present, can be retrieved from the macroscopic temperature determined at the level where no material microstructure is visible. The method used to do it is based on the solution of the independent problem, which allows to find the so-called "microstructure" functions ϕ, S. At the lowest level of approximation, corresponding to assumption of two scales (micro and macro) separation these functions do not vary in time and depend only on the way medium constituents are distributed and what are their thermal properties.

An example of application of the method was presented for steady heat flow in a composite made from two constituents. The results were found to compare well to the exact solution of the considered problem – see Fig. 3. Subsequently, the range of application of such lowest approximation of the method was studied. The theoretical considerations indicate that in this case the effective thermal conductivity should not depend on time. Therefore the variation of the effective thermal conductivity with time was investigated. Transient heat conduction with the presence and lack of phase transformation was analyzed in a fibre-reinforced composite with heat flow perpendicular to fibres. The fibre material was differently dispersed in the medium, i.e., the increasing number of fibres was considered with the total amount of fibre material unchanged. The effective thermal conductivity of the composite was determined from numerical simulations using the method corresponding to the steady state method of thermal conductivity measurement. It was found that if the long enough time of heat conduction process is considered the effective thermal conductivity attains constant, asymptotic values in agreement with the two scale approximation discussed earlier. The asymptotic values of λ_{ef} were independent of the volumetric specific heats of composite constituents, degree of fibre material dispersion or whether phase transformation was present or absent in the composite. Moreover, the asymptotic, constant values of λ_{ef} were attained for shorter times if the degree of constituent dispersion was greater. If the nondimensional time (Fourier number) based on the microdimension is introduced all the thermal conductivity curves merge to the same line for higher Fo numbers leading to asymptotic, constant value of the effective thermal conductivity value for Fo > 1. If the phase transformation is present oscillations in variation of λ_{ef}/λ_m values with time, when the effective thermal conductivity tend to its asymptotic value, were observed. These oscillations were significantly damped in time. Their origin seems to be of numerical nature. The latter conclusion was derived from the observation that when the latent heat of melting was decreased the oscillation had a lower amplitude.

Received 18 June 2014

References

[1] Banaszek J., Furmański P. and Rebow M.: *Modelling of Transport Phenomena in Cooled and Solidifying Single Component and Binary Media*. Warsow University of Technology, Warsaw 2005.

[2] Ciobanas A.I., Fautrelle Y.: *Ensemble averaged multi-phase Eulerian model for columnar/equiaxed solidification of a binary alloy: II. Simulation of the columnar-to-equiaxed transition (CET)*. J. Phys. D: Appl. Phys. **40**(2007), 4310–4336.

[3] Das S.: *Modeling mixed microstructures using a multi-level cellular automata finite element framework*. Computat. Mater. Sci. **47**(2010), 705–711.

[4] Eshraghi M., Felicelli S.D.: *An implicit lattice Boltzmann model for heat conduction with phase change*. Int. J. Heat & Mass Trans. **55**(2012), 2420–2428.

[5] Furmański P.: *Microscopic-Macroscopic Modelling of Transport Phenomena During Solidification in Heterogeneous Systems*, Courses and Lectures – No. 449 "Phase Change with Convection: Modelling and Validation", CISM Springer-Verlag 2004, 55–126.

[6] Ganapathysubramanian B., Zabaras N.: *A stochastic multi-scale framework for modeling flow through random heterogeneous porous media*. J. Comput. Phys. **228**(2009), 591–618.

[7] Mishra S.M., Behera N.C., Garg A.K., Mishra A.: *Solidification of a 2-D semitransparent medium using the lattice Boltzmann method and the finite volume method*. Int. J. Heat Mass Tran. **51**(2008), 4447–4460.

[8] Ruan Ch., Ouyang J., Liu Sh.: *Multi-scale modeling and simulation of crystallization during cooling in short fiber reinforced composites*. Int. J. Heat Mass Tran. **55**(2012), 1911–1921.

[9] Sanyal D., Ramachandrarao P., Gupta O.P.: *A fast strategy for simulation of phase change phenomena at multiple length scales*. Comput. Mater. Sci. **37**(2006), 166–177.

[10] Tan L., Zabaras N.: *Multi-scale modeling of alloy solidification using a database approach*. J. Comput. Phys. **227**(2007), 728–754.

[11] WangJ.-L., Wang F.-M., Zhao Y.-Y., Zhang J.-M., Ren W.: *Numerical simulation of 3D-microstructures in solidification processes based on the CAFE method*. Int. J. Miner. Metall. Mater. **16**(2009), 640–645.

[12] Zeng Q.H., Yu A.B., Lu G.Q.: *Multi-scale modeling and simulation of polymer nano-composites*. Prog. Polym. Sci. **33**(2008), 191–269.

[13] ANSYS FLUENT version 14.0.